

## Autopresentation of scientific accomplishments (autoreferat)

### I. NAME

Jakub Wagner

### II. DEGREES

**2008:** PhD in theoretical physics, *Electroweak Symmetry Breaking and the Structure of Radiative Corrections in Extensions of the Standard Model*, University of Warsaw, Faculty of Physics, supervisor: P.H.Chankowski

**2002:** M.Sc. in the field of theoretical Particle Physics, University of Warsaw, Faculty of Physics, supervisor: P.H.Chankowski

### III. EMPLOYMENT IN ACADEMIC INSTITUTIONS

**2008 - present:** Narodowe Centrum Badań Jądrowych, position: assistant professor

### IV. SCIENTIFIC ACHIEVEMENT, IN THE SENSE OF ARTICLE 16, PARAGRAPH 2 OF THE ACT ON ACADEMIC DEGREES AND ACADEMIC TITLE AND DEGREES AND TITLE IN ART (DZ. U. NR 65, POZ. 595 ZE ZM.)

#### A. Title of the scientific achievement - a monographic series of publications:

*Study of exclusive processes with large timelike scales*

#### B. The monographic series of publications (given in chronological order)

**S1:** *Can one measure timelike Compton scattering at LHC?*

B. Pire, L. Szymanowski, J. Wagner

Published in **Phys.Rev.D79** (2009) 014010

**S2:** *NLO corrections to timelike, spacelike and double deeply virtual Compton scattering*

B. Pire, L. Szymanowski, J. Wagner

Published in **Phys.Rev.D83** (2011) 034009

**S3:** *On timelike and spacelike hard exclusive reactions*

D. Mueller, B. Pire, L. Szymanowski, J. Wagner

Published in **Phys.Rev.D86** (2012) 031502

**S4:** *Timelike and spacelike deeply virtual Compton scattering at next-to-leading order*

H. Moutarde, B. Pire, F. Sabatié, L. Szymanowski, J. Wagner

Published in **Phys.Rev.D87** (2013) 054029

**S5:** *Timelike Compton scattering with a linearly polarized photon beam*

A.T. Goritschnig, B. Pire, J. Wagner

Published in **Phys.Rev.D89** (2014) 094031

**S6:** *Lepton-pair production in ultraperipheral collisions at AFTER@LHC*

J.P. Lansberg, L. Szymanowski, J. Wagner

Published in **JHEP 1509** (2015) 087

**S7:** *Hard photoproduction of a diphoton with a large invariant mass*

A. Pędrak, B. Pire, L. Szymanowski, J. Wagner

Published in **Phys.Rev.D96** (2017) 074008

**C. Descriptions of scientific goal of the monographic series of publications and the results achieved and a description of possible applications of the results**

*1. Introduction*

Understanding the structure of nucleons in terms of the elementary building blocks of quantum chromodynamics, *i.e.* quarks and gluons, is among the most important questions of high energy physics. During the past few decades the main effort to solve that problem focused mostly on the inclusive scattering, in which properties of only some of the final particles are measured. Among those processes the most important is Deep Inelastic Scattering

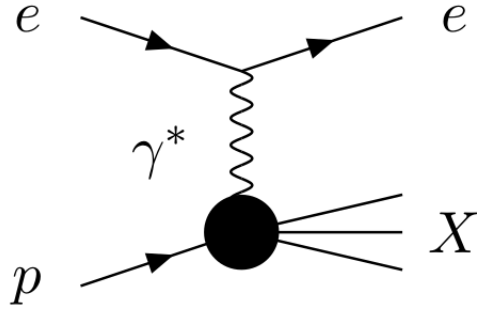


FIG. 1. Deep Inelastic Scattering (DIS)

(DIS) of electrons on protons:

$$e(k) + p(p) \rightarrow e(k') + X, \quad (1)$$

where one does not measure properties of the resulting hadronic system  $X$ , but only the momentum  $k'$  of the scattered electron. This process is illustrated with Fig.1. In the Björken limit i.e. when both photon virtuality  $Q^2 = -q^2 \equiv (k - k')^2$  and squared hadronic c.m. energy  $(p + q)^2$  become large, with the ratio  $x_B = \frac{Q^2}{2p \cdot q}$  fixed, the cross section factorizes into a hard partonic subprocess that is calculable in the perturbation theory, and Parton Distribution Functions (PDF):

$$\sigma = \text{PDF} \otimes \text{partonic cross section} \quad (2)$$

PDFs encode information about distribution of longitudinal momentum and polarization carried by quarks, antiquarks and gluons in hadron, but do not provide any information on how partons are distributed in the transverse plane and how important is the orbital angular momentum component in making up the spin of nucleon. However, during the last twenty years we have witnessed a very active progress in addressing this issues due to the discovery of Generalized Parton Distributions (GPDs) and their role in the description of hard exclusive processes [1–5]. The simplest such process, and the best known from experimental and theoretical perspectives is Deeply Virtual Compton Scattering (DVCS) (shown in Fig.2):

$$e(k) + p(p) \rightarrow e(k') + p(p') + \gamma(q') \quad . \quad (3)$$

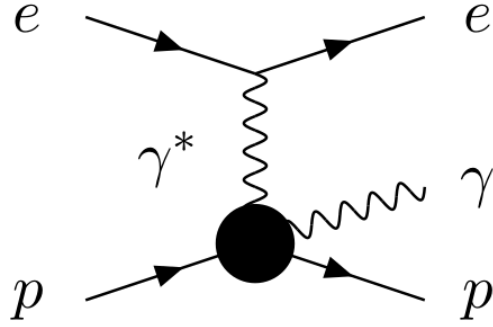


FIG. 2. Deeply Virtual Compton Scattering (DVCS).

This process is conveniently described in terms of symmetric variables:

$$P = \frac{p + p'}{2} \quad , \quad \bar{q} = \frac{q + q'}{2} \quad , \quad (4)$$

which can be used to define the generalized Björken variable  $\xi$ :

$$\xi = \frac{-\bar{q}^2}{2\bar{q} \cdot P} \approx \frac{x_B}{2 - x_B} \quad , \quad \text{where:} \quad x_B = \frac{Q^2}{2q \cdot p} \quad . \quad (5)$$

In the convenient reference frame, where  $P$  has only positive time- and  $z$ -components, and light vectors are defined as:

$$v_+ = (1, 0, 0, 1) \frac{1}{\sqrt{2}} \quad , \quad v_- = (1, 0, 0, -1) \frac{1}{\sqrt{2}} \quad , \quad (6)$$

$(-2\xi)$  has an interpretation of the fraction of momentum transport in "+" direction. Another important variable is the square of momentum transfer between incoming and outgoing proton:

$$t = (p' - p)^2. \quad (7)$$

In the generalized Björken limit DVCS amplitude factorizes into generalized parton distributions (GPDs) and perturbative coefficient functions (given by partonic amplitude):

$$\mathcal{M} = \text{GPD} \otimes \text{partonic amplitude} .$$

Formal definition of GPDs is given by matrix elements of appropriate light-cone operators.

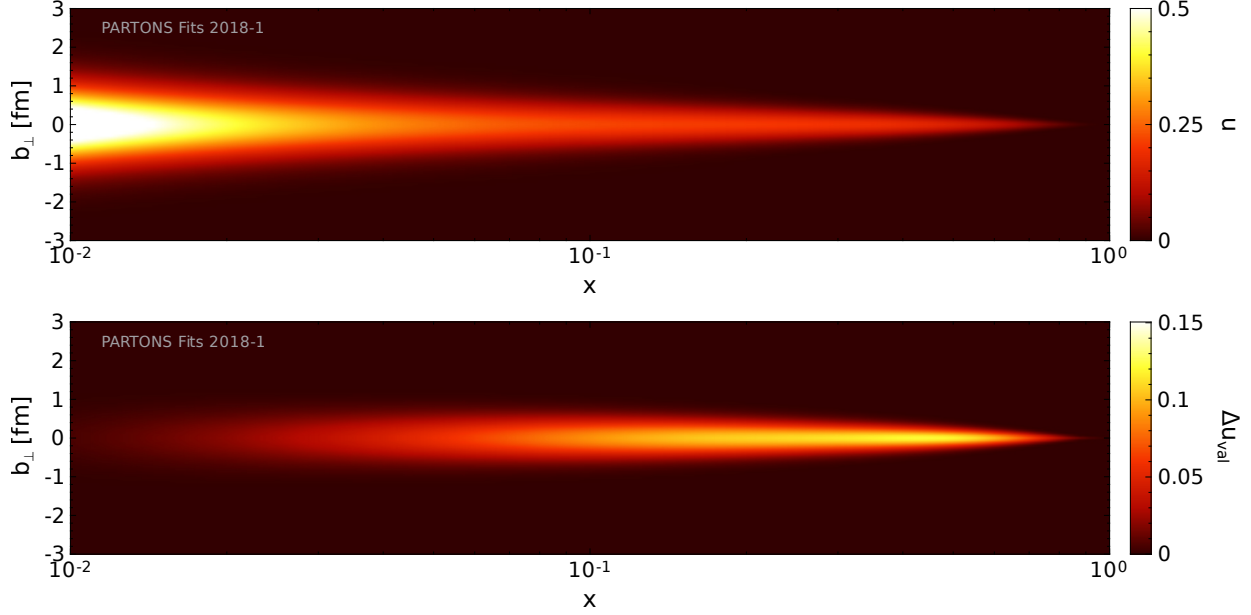


FIG. 3. Position of up quarks in an unpolarized proton (upper plot) and longitudinal polarization of those quarks in a longitudinally polarized proton (lower plot) as a function of the longitudinal momentum fraction  $x$ . For the lower plot only the valence contribution is shown. The plot from reference [P4].

Below we give the example of so-called vector GPDs, for quark ( $F^q$ ) and gluons ( $F^g$ ):

$$\begin{aligned}
F^q(x, \xi, t) &= \frac{1}{2} \int \frac{dz^-}{2\pi} e^{ixP^+z^-} \langle p' | \bar{q}(-\frac{1}{2}z) \gamma^+ q(\frac{1}{2}z) | p \rangle \Big|_{z^+=0, \mathbf{z}=0} \\
&= \frac{1}{2P^+} \left[ H^q(x, \xi, t) \bar{u}(p') \gamma^+ u(p) + E^q(x, \xi, t) \bar{u}(p') \frac{i\sigma^{+\alpha} \Delta_\alpha}{2m} u(p) \right], \\
F^g(x, \xi, t) &= \frac{1}{P^+} \int \frac{dz^-}{2\pi} e^{ixP^+z^-} \langle p' | G^{+\mu}(-\frac{1}{2}z) G_\mu^+(\frac{1}{2}z) | p \rangle \Big|_{z^+=0, \mathbf{z}=0} \\
&= \frac{1}{2P^+} \left[ H^g(x, \xi, t) \bar{u}(p') \gamma^+ u(p) + E^g(x, \xi, t) \bar{u}(p') \frac{i\sigma^{+\alpha} \Delta_\alpha}{2m} u(p) \right].
\end{aligned}$$

Comparing to inclusive PDFs, GPDs are functions of two additional variables -  $\xi$  and  $t$  - which on the one hand reflects the advantage of carrying much more information on the hadron structure, but on the other makes it much more difficult to extract them from the experimental data.

Two features of GPDs attracted most attention: their relation to the total angular momentum of partons [2, 3], allowing to solve the proton's spin puzzle, and the information about to position of quarks and gluons in the plane transverse to the direction of proton's

motion [6–8], allowing for the so-called "hadron tomography". The first feature is usually summarized by the Ji sum rule:

$$\lim_{t \rightarrow 0} \int_{-1}^1 dx x [H_q(x, \xi, t) + E_q(x, \xi, t)] = 2J_q$$

where  $J_q$  is fraction of the proton spin carried by quark  $q$  (including spin and orbital angular momentum). The hadronic tomography is possible thanks to the fact that at  $\xi \rightarrow 0$  limit the variable  $t$  reduces to the transverse momentum transfer squared i.e.  $-t \rightarrow \Delta_{\perp}^2$ , and the Fourier transform of GPD  $H$ :

$$H(x, \mathbf{b}_{\perp}) = \int \frac{d^2 \Delta_{\perp}}{(2\pi)^2} e^{-i\mathbf{b}_{\perp} \cdot \Delta_{\perp}} H(x, 0, -\Delta_{\perp})$$

can be interpreted as probability of finding a parton with longitudinal momentum fraction  $x$  at a given impact parameter  $\mathbf{b}_{\perp}$ . On the Fig. 3 we have shown an example of such a probability-density plot extracted from the DVCS data in our recent study [9].

After exploratory experiments on Deeply Virtual Compton Scattering (DVCS) and Deeply Virtual Meson Production (DVMP) [10]:

$$e(k) + p(p) \rightarrow e(k') + p(p') + M(q') \quad , \quad (8)$$

in JLab, DESY and CERN, and almost 20 years of theoretical effort, the effectiveness of the GPD formalism has been proven [11, 12]. Nowadays, the measurements of exclusive processes are among the main goals of the experimental programmes carried out by the new generation of experiments - those already running, like Hall-A with CLAS at JLab upgraded to 12 GeV [13] and COMPASS-II at CERN[14], and those foreseen in the future, like Electron Ion Collider (EIC) [15] and Large Hadron Electron Collider (LHeC) [16].

In the **presented monographic series of publications**, I was studying the processes with a large timelike scale, mostly focusing on the Timelike Compton Scattering (TCS) i.e. process of the photoproduction of lepton pairs [17]:

$$\gamma(q) + P(p) \rightarrow P(p') + l^+(k) + l^-(k') \quad , \quad (9)$$

illustrated in Fig. 4. Such a process is of great interest, because of its complementarity to DVCS. Contrary to DVMP, where in the calculation of amplitudes one has to take into account also a nonperturbative object describing the formation of meson - poorly known distribution amplitude (DA) - in DVCS and TCS the only nonperturbative objects are GPDs

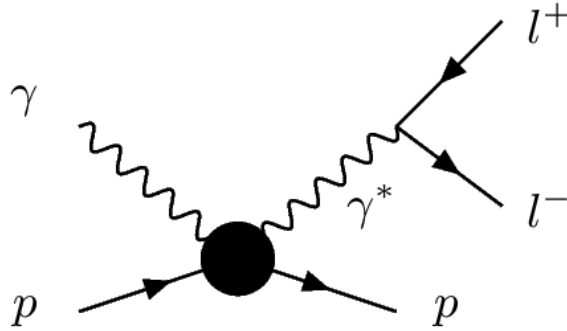


FIG. 4. Timelike Compton Scattering (TCS).

itself. This property makes TCS best candidate to prove the universality of the GPD formalism. However such a universality check can only be meaningful if the next-to-leading order (NLO) corrections in the strong coupling are taken into account. The analytical structure of those corrections is very different in the processes with a large timelike and spacelike scales. Appearance of the large timelike scale enables the production of intermediate states in some channels which were kinematically forbidden in the spacelike case. This opens the way to new absorptive parts of the amplitude. Former experience with inclusive deep reactions also teaches us that NLO corrections are likely to be more important in timelike reactions than in the corresponding spacelike ones. The well-known example of the Drell Yan K-factor teaches us that NLO corrections are sizeable in timelike processes, because of  $i\pi$  factors coming from  $\log(-Q^2/\mu_F^2)$  terms, which often exponentiate when soft gluon resummation is taken care of [18, 19].

The presented series of publications constitutes complete and thorough study of hard exclusive processes with large timelike scales, starting from the derivation of NLO formulae for the amplitudes, through studies of their phenomenological implications, up to the predictions for measurements at specific experimental facilities. It is worth stressing that it led also to the co-authorship of the approved proposals for the experiments at the Thomas Jefferson National Accelerator Facility (JLAB):

[www.jlab.org/exp\\_prog/proposals/12/PR12-12-001.pdf](http://www.jlab.org/exp_prog/proposals/12/PR12-12-001.pdf)

[www.jlab.org/exp\\_prog/proposals/15/PR12-12-006A.pdf](http://www.jlab.org/exp_prog/proposals/15/PR12-12-006A.pdf)

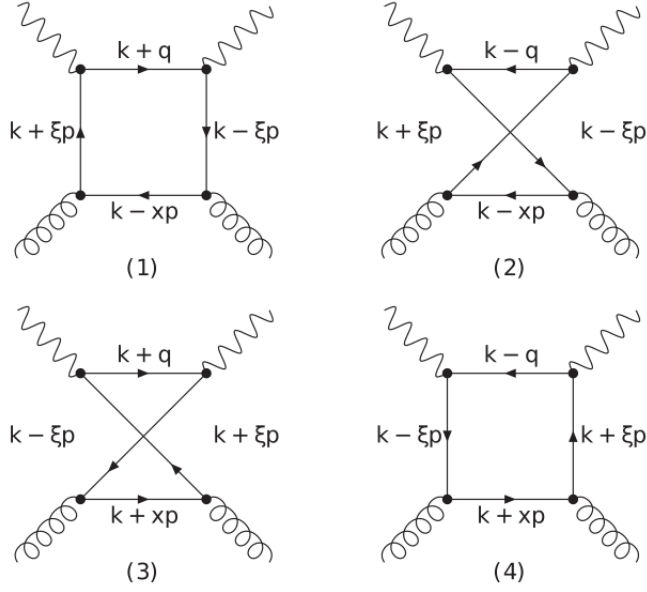


FIG. 5. First group of diagrams describing  $\gamma g \rightarrow \gamma g$  scattering.

The monographic series, and hence this report, about processes with timelike scales consists of the following topics: i) derivation and study of the analytic structure of the NLO amplitude of the spacelike and timelike processes (references [S2] and [S3]), ii) numerical study of NLO corrections for DVCS and TCS (reference [S4]), iii) proposals of new experimental possibilities for measurements of such processes (references [S1], [S5] and [S6]) and finally iv) proposal (Ref. [S7]) of a new process of the photoproduction of a photons pair with large invariant mass, which also depends on large timelike scale and can be measured at JLAB.

## 2. Analytic structure of the amplitude at the NLO

In the reference [S2] we have calculated the  $O(\alpha_s)$  corrections to the amplitude of Double Deeply Virtual Compton scattering (DDVCS):

$$\gamma^*(q_{in}) + p(p) \rightarrow \gamma^*(q_{out}) + p'(p). \quad (10)$$

This general result was then used to derive formulae for the limiting cases of  $q_{out}^2 = 0$  and  $q_{in}^2 = 0$ , corresponding to DVCS and TCS processes, respectively. Phenomenology of

DDVCS has been discussed in Ref. [20].

Our motivation for this study comes from the fact, that historically, the understanding of inclusive reactions (Drell Yan reactions, large  $p_T$  hadron or jet production) in the framework of collinear QCD factorization has waited for an analysis including next-to-leading order (NLO) (or even next-to-next-to-leading order) corrections. Indeed, complete NLO calculations [21–24] were available for DVCS reaction and there was no indication that they are negligible in the kinematics relevant for current or near future experiments. This was likely to be even more the case for TCS. Amplitudes of TCS and DVCS are identical (up to a complex conjugation) at lowest order in  $\alpha_S$ , but differ at next to leading order, in particular because of a different analytic structure of these reactions.

It is customary to parametrize the amplitude (here for simplicity we show only its symmetric part) in terms of Compton Form Factors (CFFs, here denoted by  $\mathcal{H}$  and  $\mathcal{E}$ ):

$$\mathcal{A}^{\mu\nu} = -e^2 \frac{1}{(P+P')^+} \bar{u}(P') \left[ g_T^{\mu\nu} \left( \mathcal{H} \gamma^+ + \mathcal{E} \frac{i\sigma^{+\rho} \Delta_\rho}{2M} \right) \right] u(P). \quad (11)$$

According to factorization theorems, CFFs are given by convolutions of coefficients functions ( $T^q$  for quarks and  $T^g$  for gluons) with GPDs:

$$\begin{aligned} \mathcal{H} &= \int_{-1}^1 dx \left( \sum_q T^q H^q + T^g H^g \right), \\ \mathcal{E} &= \int_{-1}^1 dx \left( \sum_q T^q E^q + T^g E^g \right). \end{aligned} \quad (12)$$

Our calculation was performed in  $\overline{MS}$  scheme, with dimension  $D = 4 + \epsilon$  regularizing infrared divergences, as all ultraviolet divergences cancel out. We have described the one-

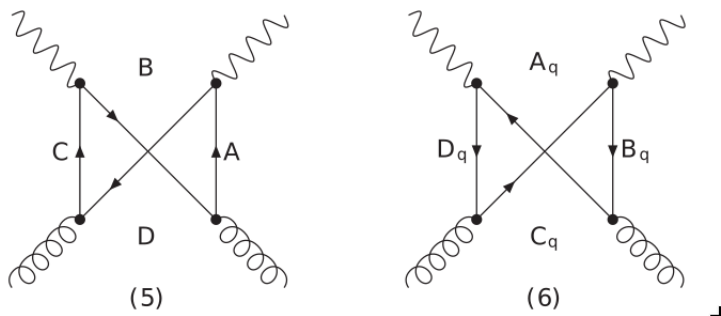


FIG. 6. Second group of diagrams describing  $\gamma g \rightarrow \gamma g$  scattering.

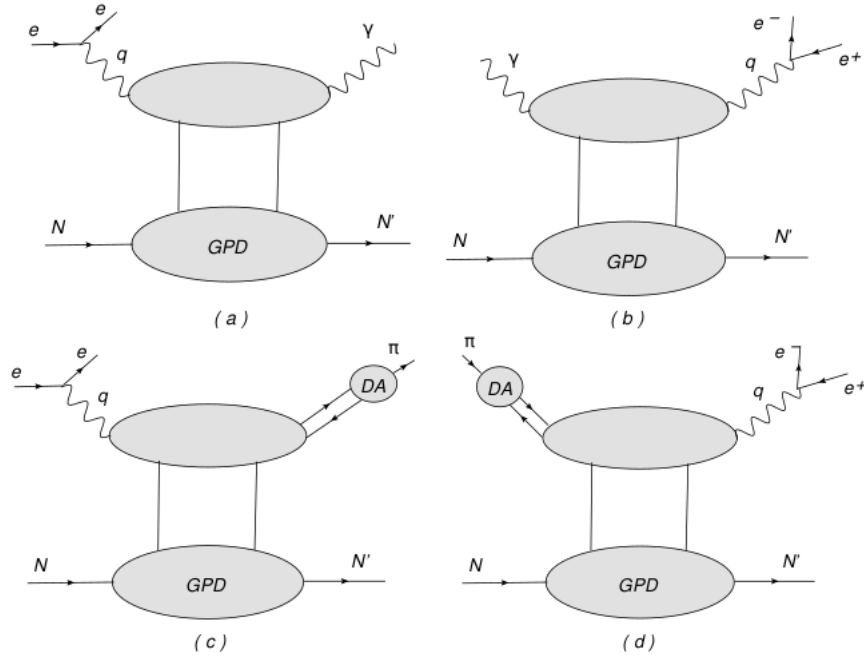


FIG. 7. The DVCS (a) and TCS (b) processes, as well as meson electroproduction (c) and exclusive Drell Yan in  $\pi N$  collisions (d) are linked by time reversal and analyticity. They factorize in hard coefficients (upper blob), generalized parton distributions (lower blob) and distribution amplitudes (c,d).

loop calculations (diagrams corresponding to gluonic GPDs are presented in Figs. 5 and 6) necessary to obtain the needed coefficient functions, in great details, as they can be useful in the calculations of similar exclusive processes. Main results are summarized in Eqs. (46 and 47) for the general case of DDVCS, and then in the special cases of DVCS (TCS) in Eq. 48 and 49 (respectively 50 and 51). They are in agreement with earlier results [21, 22], which were obtained in an unphysical region of parameter space, and then analytically continued to obtain DVCS case (which is possible due to simple analytic structure of hard DVCS amplitude). The results for NLO corrections to DDVCS and TCS were calculated for the first time, and laid the ground for phenomenological applications, some of which were performed in the papers included in the presented monographic series, and are described below.

In the reference [S3] we have generalized the result obtained in [S2], obtaining the general relation between amplitudes of processes with large spacelike and timelike hard scale at

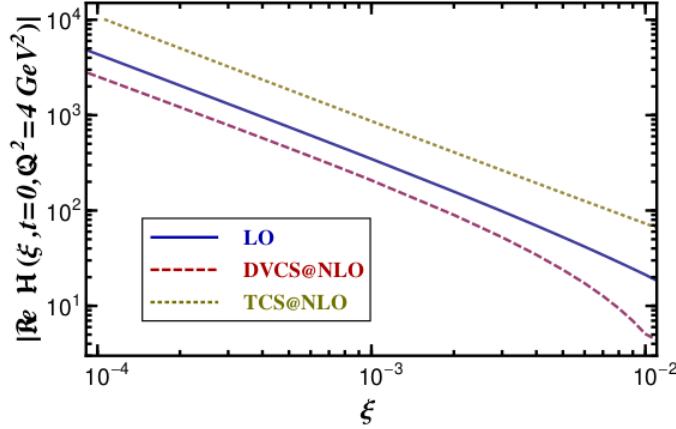


FIG. 8. The real part of CFF  $\mathcal{H}$  vs.  $\xi$  with  $\mu^2 = Q^2 = 4 \text{ GeV}^2$  and  $t = 0$  at LO (solid) and NLO for DVCS (dashed). For TCS at NLO its negative value is shown as dotted curve.

NLO accuracy. We illustrated this relation on examples of electroproduction of a photon or meson, and photo- or meso-production of a lepton pair (see Fig. 7). We have shown that the factorization property of exclusive amplitudes at leading twist together with analyticity allow to link Compton Form Factors in the *timelike* ( ${}^T\mathcal{H}$ ) and *spacelike* ( $\mathcal{H}$ ) cases:

$${}^T\mathcal{H} \stackrel{\text{NLO}}{=} \mathcal{H}^* - i\pi Q^2 \frac{\partial}{\partial Q^2} \mathcal{H}^*, \quad (13)$$

$${}^T\tilde{\mathcal{H}} \stackrel{\text{NLO}}{=} -\tilde{\mathcal{H}}^* + i\pi Q^2 \frac{\partial}{\partial Q^2} \tilde{\mathcal{H}}^*. \quad (14)$$

An analog relation connects timelike  $\pi^\pm$  with spacelike  $\pi^\mp$  transition form factors (TFFs), as shown in Eq. 27 of [S3].

The NLO relations (13–14) tell us that if scaling violations are small, the timelike CFFs (TFFs) can be obtained from the spacelike ones by complex conjugations. Moreover, GPD model studies indicate that in the valence region, i.e. for  $\xi \sim 0.2$ , CFFs might only evolve mild. On the other hand it is known that the evolution of CFF  $\mathcal{H}$  in the small  $\xi$  region induces that the imaginary part  $\Im\mathcal{H}$  dominates over the real one  $\Re\mathcal{H}$ , which is consistent with a phenomenological analysis of HERA data [25]. Since of the  $-i\pi$  proportional NLO addenda in (13), the small  $\Re\mathcal{H}$  will only mildly influence the LO prediction  $\Im\mathcal{H} \stackrel{\text{LO}}{=} -\Im\mathcal{H}$ . On the other hand we expect huge NLO corrections to  $\Re\mathcal{H} \stackrel{\text{LO}}{=} \Re\mathcal{H}$ , induced by  $\Im\mathcal{H}$ . Utilizing Goloskokov-Kroll model for  $H$  GPDs [26], we illustrate this effect in Fig. 8 for  $10^{-4} \leq \xi \leq 10^{-2}$ , accessible in a suggested Electron-Ion-Collider [27], and  $t = 0$ . We plot  $\Re\mathcal{H}$  vs.  $\xi$ , for LO DVCS or TCS (solid), NLO DVCS (dashed) and NLO TCS (dotted)

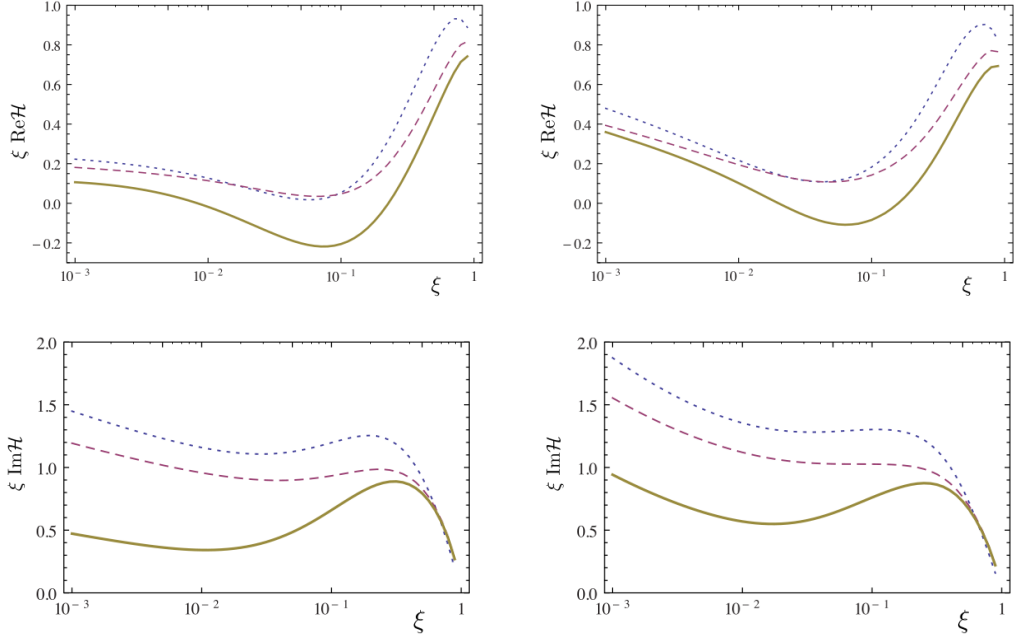


FIG. 9. The real (upper line) and imaginary (lower line) parts of the *spacelike* Compton Form Factor  $\mathcal{H}(\xi)$  multiplied by  $\xi$ , as a function of  $\xi$  in the double distribution model based on Kroll-Goloskokov (left column) and MSTW08 (right column) parametrizations, for  $\mu_F^2 = Q^2 = 4 \text{ GeV}^2$  and  $t = -0.1 \text{ GeV}^2$ , at the Born order (dotted line), including the NLO quark corrections (dashed line) and including both quark and gluon NLO corrections (solid line).

at the input scale  $\mu^2 = Q^2 = 4 \text{ GeV}^2$ . In the case of NLO TCS  $-\Re^T \mathcal{H}$  is shown, since even the sign changes. We note that the NLO correction to  $\Re^T \mathcal{H}$  is of the order of  $-400\%$  and so the real part in TCS becomes of similar importance as the imaginary part. This NLO prediction is testable via a lepton-pair angle asymmetry, governed by  $\Re^T \mathcal{H}$  [17]. Such drastic effect of the timelike nature of outgoing photon was also found in the dipole model approach [28]. More detailed study of the phenomenological consequences was a subject of the reference [S4].

### 3. Phenomenological consequences

In the reference [S4], using the results obtained in papers [S2] and [S3], we have studied the phenomenological consequences of the NLO corrections to the amplitudes and observables in DVCS and TCS, focusing on kinematics relevant to the JLab12 and COMPASS mea-

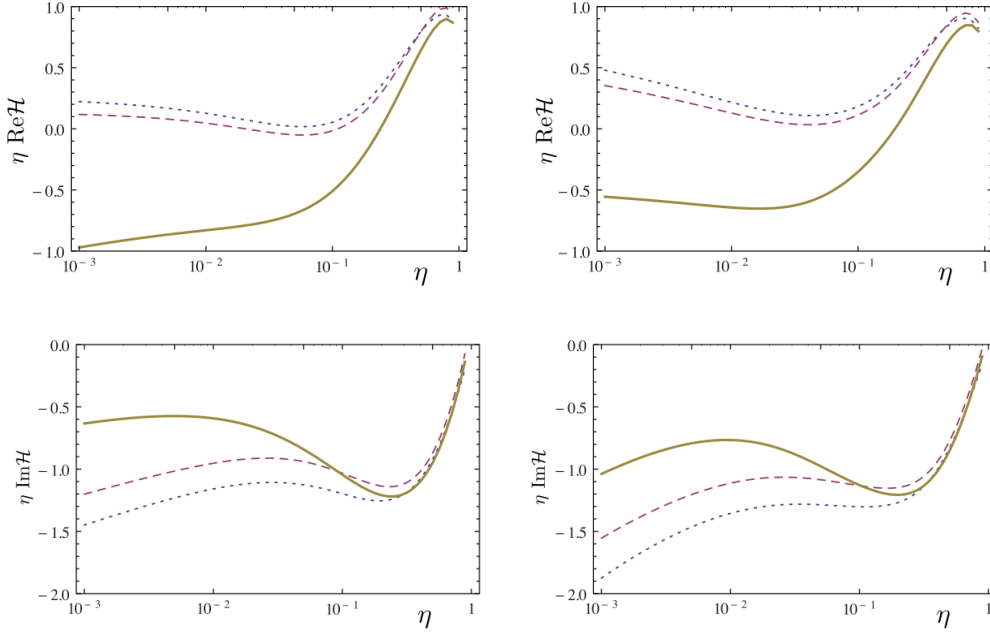


FIG. 10. The real (upper line) and imaginary (lower line) parts of the *timelike* Compton Form Factor  $\mathcal{H}(\eta)$  multiplied by  $\eta$ , as a function of  $\eta$  in the double distribution model based on Kroll-Goloskokov (left column) and MSTW08 (right column) parametrizations, for  $\mu_F^2 = Q^2 = 4 \text{ GeV}^2$  and  $t = -0.1 \text{ GeV}^2$ , at the Born order (dotted line), including the NLO quark corrections (dashed line) and including both quark and gluon NLO corrections (solid line). Parameter  $\eta$  denotes the skewness in the TCS process.

measurements. To estimate the consequence of including NLO gluon coefficient functions and NLO corrections to the quark coefficient functions quantitatively, we adopted two models of GPDs, based on the so-called double distributions (DDs) [29, 30]. DDs allow to trivially achieve one of the strongest constraints on GPDs : the polynomiality of the Mellin moments of GPDs. They also automatically restore usual PDFs in the forward limit at  $\xi, t \rightarrow 0$ . First model is the so-called Goloskokov-Kroll (or GK) [12, 26, 31, 32], second - the simple factorized model based on the MSTW08 PDFs [33].

We have demonstrated, in the case of medium energy kinematics to be explored in the near future at JLab and by COMPASS, that the inclusion of NLO corrections is an important issue, and that the difference of those corrections between spacelike and timelike regimes is so sizeable that it can be promoted to the status of direct tests of the QCD understanding

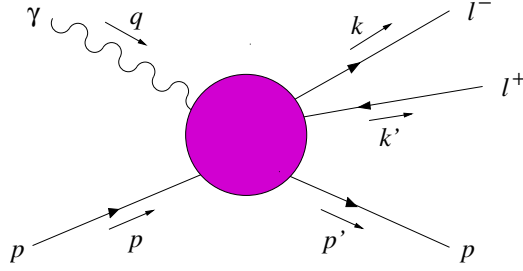


FIG. 11. Real photon-proton scattering into a lepton pair and a proton.

of the reactions (see Fig.9 for a DVCS and Fig.10 for TCS Compton Form Factors).

The physical process where to observe TCS is photoproduction of a heavy lepton pair,  $\gamma N \rightarrow \mu^+\mu^- N$  or  $\gamma N \rightarrow e^+e^- N$ , shown in Fig. 11. As in the case of DVCS, Bethe-Heitler (BH) mechanism – sometimes called  $\gamma\gamma$  process since the lepton pair is produced through the  $\gamma\gamma \rightarrow \ell^+\ell^-$  subprocess – contributes at the amplitude level. This amplitude is completely calculable in QED provided one knows the Nucleon Form Factors at small  $t$ . This process has a very peculiar angular dependence and overdominates the TCS process if one blindly integrates over the final phase space. One may however choose kinematics where the amplitudes of the two processes are of the same order of magnitude, and either subtract the well-known Bethe-Heitler process or use specific observables sensitive to the interference of the two amplitudes.

The kinematics of the  $\gamma(q)N(p) \rightarrow \ell^-(k)\ell^+(k')N(p')$  process is shown in Fig. 12. In the  $\ell^+\ell^-$  center of mass system, one introduces the polar and azimuthal angles  $\theta$  and  $\varphi$  of  $\vec{k}$ , with reference to a coordinate system with 3-axis along  $-\vec{p}'$  and 1- and 2-axes such that  $\vec{p}$  lies in the 1-3 plane and has a positive 1-component.

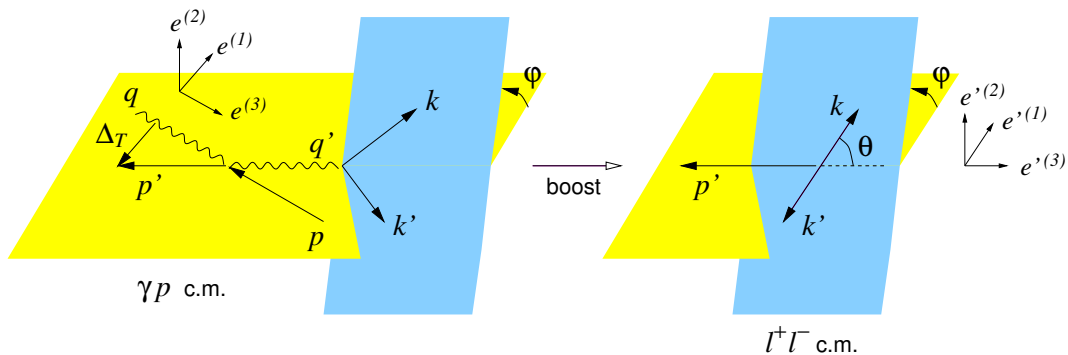


FIG. 12. Kinematical variables and coordinate axes in the  $\gamma p$  and  $\ell^+\ell^-$  c.m. frames.

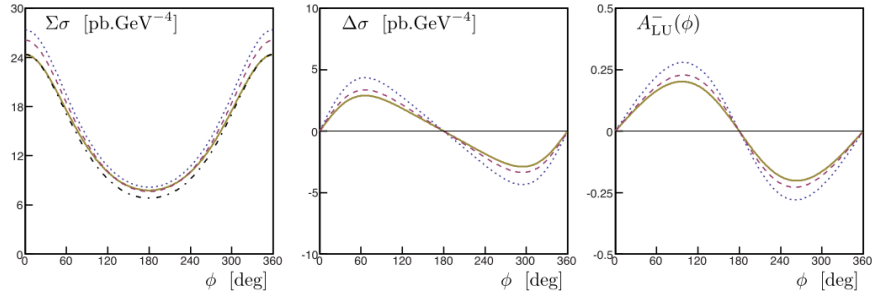


FIG. 13. From left to right, the total DVCS cross section in  $\text{pb}/\text{GeV}^4$ , the difference of cross sections for opposite lepton helicities in  $\text{pb}/\text{GeV}^4$ , the corresponding asymmetry, all as a function of the usual  $\phi$  angle (in the Trento convention [34]) for  $E_e = 11 \text{ GeV}$ ,  $\mu_F^2 = Q^2 = 4 \text{ GeV}^2$  and  $t = -0.2 \text{ GeV}^2$ . The GPD  $H(x, \xi, t)$  is parametrized by the GK model and the contributions from other GPDs are not included. In all plots, the LO result is shown as the dotted line, the full NLO result by the solid line and the NLO result without the gluonic contribution as the dashed line. The Bethe-Heitler contribution appears as the dash-dotted line in the cross section plots (left part).

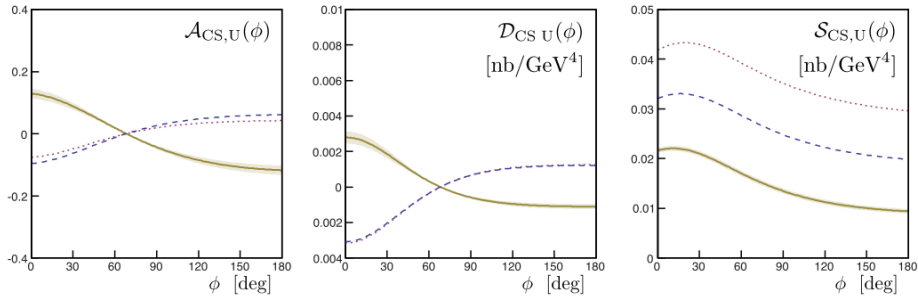


FIG. 14. The DVCS observables for the COMPASS experiment, from left to right, mixed charge-spin asymmetry, mixed charge-spin difference and mixed charge-spin sum (in  $\text{nb}/\text{GeV}^4$ ). The kinematical point is chosen as  $\xi = 0.05$ ,  $Q^2 = 4 \text{ GeV}^2$ ,  $t = -0.2 \text{ GeV}^2$ . The GPD  $H(x, \xi, t)$  is parametrized by the double distribution model based on the MSTW08 parametrization. The contributions from other GPDs are not included. In all plots, the LO result is shown as the dotted line, the full NLO result by the solid line and the NLO result without the gluonic contribution as the dashed line.

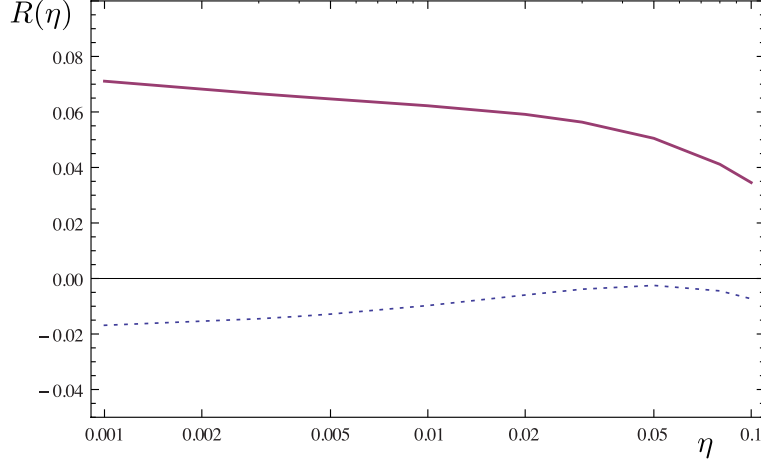


FIG. 15. Ratio  $R$  defined by Eq. (15) as a function of  $\eta$ , for  $Q^2 = \mu_F^2 = 4 \text{ GeV}^2$  and  $t = -0.1 \text{ GeV}^2$ . The dotted line represents LO contribution and the solid line represents NLO result.

We have illustrated the discussed effect of NLO corrections with predictions for several observables accessible in DVCS and TCS measurements. In Fig. 13 we have presented the beam spin asymmetry for DVCS process and JLAB12 kinematics, and in Fig.14 – the mixed charge-spin asymmetry for DVCS process, relevant for COMPASS experiment. In the case of TCS to quantify how big is the deviation from pure Bethe-Heitler process in the unpolarized cross section we calculate (see Fig. 15) the ratio  $R$  defined in Ref. [17] by

$$R(\eta) = \frac{2 \int_0^{2\pi} d\varphi \cos \varphi \frac{dS}{dQ'^2 dt d\varphi}}{\int_0^{2\pi} d\varphi \frac{dS}{dQ'^2 dt d\varphi}}, \quad (15)$$

where  $S$  is a weighted cross section given by Eq. (43) of Ref. [17]. It is plotted in Fig. 15 as a function of the skewness  $\eta$  for  $Q^2 = \mu^2 = 4 \text{ GeV}^2$  and  $t = -0.2 \text{ GeV}^2$ . In the leading twist the numerator of Eq. 15 is linear in the real part of CFFs, and the denominator, for the kinematics we consider, is dominated by the Bethe-Heitler contribution. The inclusion of NLO corrections to the TCS amplitude is indeed dramatic for such an observable and includes also the change of sign.

Imaginary parts of the TCS CFFs are accesible through observables making use of photon circular polarizations [17]. The photon beam circular polarization asymmetry

$$A = \frac{\sigma^+ - \sigma^-}{\sigma^+ + \sigma^-}, \quad (16)$$

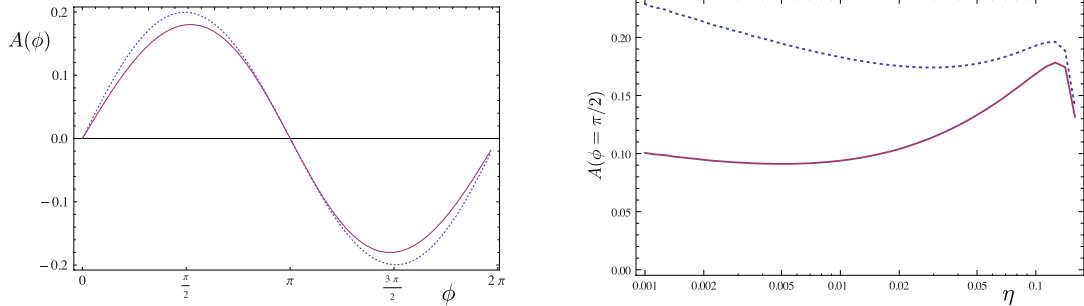


FIG. 16. (Left) Photon beam circular polarization asymmetry as a function of  $\phi$ , for  $t = -0.1 \text{ GeV}^2$ ,  $Q^2 = \mu^2 = 4 \text{ GeV}^2$ , integrated over  $\theta \in (\pi/4, 3\pi/4)$  and for  $E_\gamma = 10 \text{ GeV}$  ( $\eta \approx 0.11$ ). (Right) The  $\eta$  dependence of the photon beam circular polarization asymmetry for  $Q^2 = \mu^2 = 4 \text{ GeV}^2$ , and  $t = -0.2 \text{ GeV}^2$  integrated over  $\theta \in (\pi/4, 3\pi/4)$ . The LO result is shown as the dotted line, the full NLO result by the solid line.

is shown in the left part of Fig. 16, as a function of  $\phi$  for the kinematic variables relevant for JLab:  $Q^2 = 4 \text{ GeV}^2 = \mu_F^2$ ,  $t = -0.1 \text{ GeV}^2$  and  $E_\gamma = 10 \text{ GeV}$  (which corresponds to the value of skewness  $\eta \approx 0.11$ ). The same quantity is shown in the right panel of Fig. 16 as a function of  $\eta$  for  $\phi = \pi/2$  and  $Q^2 = 4 \text{ GeV}^2 = \mu_F^2$ . The effect of NLO corrections on that observable is rather large, ranging from 10% at  $\eta = 0.1$  (relevant for JLab) through 30% at  $\eta = 0.05$  (relevant for COMPASS) up to 100% at very small values of  $\eta$ .

Let us stress a feature that was largely overlooked in previous studies, namely the importance of gluon contributions to the DVCS amplitude, even when the skewness variable  $\xi$  is in the so-called valence region. This is not a real surprise when one recalls that gluons (in terms of distribution functions) are by no means restricted to the very low  $x$  region and that gluon CFFs at a given  $\xi$  value also depend on gluon PDFs at lower values of  $x$ . This effect is particularly big when one considers the real part of CFFs in the timelike case. This promotes the observables related to this quantity as sensitive probes of the 3-dimensional gluon content of the nucleon.

#### 4. Predictions for experiments

Another part of results included in the presented series of publications consists of predictions for measurements performed at present and future experimental facilities. In reference

[S4], which was described in the previous sections we have included predictions for JLAB (Fig. 13) and COMPASS (Fig. 14) experiments.

In reference [S5] we have proposed a new way of accessing the polarized GPDs  $\tilde{H}$  and  $\tilde{E}$  in TCS. Because accessing the polarized GPDs through pseudoscalar meson deep lepton production turns out to be more difficult than anticipated, TCS may be a better tool to access them if proper observables are measured. For that purpose we have considered the use of linearly polarized photon beam.

Experimental techniques have recently been developed to yield a linearly polarized, intense photon beam at JLab, using a forward tagger to detect electrons scattered at very small angles at CLAS12 [35] or using coherent bremsstrahlung technique at the GlueX experiment [36]. We have shown that this will allow for new tests of the polarized quark and gluon GPDs. A careful analysis of the angular dependence of the cross section in the angle  $\Phi_h$  between the polarization vector and the hadronic plane, allows for the definition of variable  $C$  (Eqs. 13-15 of [S5]) being sensitive to the poorly known GPD  $\tilde{H}$ :

$$C = \frac{2 - 3\pi \operatorname{Re} \left[ \mathcal{H}F_1 - \frac{t}{4M^2} \mathcal{E}F_2 - \eta \tilde{\mathcal{H}}(F_1 + F_2) \right]}{2 + \pi \operatorname{Re} \left[ \mathcal{H}F_1 - \frac{t}{4M^2} \mathcal{E}F_2 + \eta \tilde{\mathcal{H}}(F_1 + F_2) \right]}. \quad (17)$$

In order to illustrate the dependence of proposed observable on  $\tilde{H}$  we made use of Goloskokov-Kroll GPDs model. We presented our numerical estimates with the GPD  $E$  set to zero, as it is largely unknown and also suppressed by the small kinematic factor  $\frac{t}{4M^2}$ . On the left-hand side of figure 17 we present the ratio  $C$  as a function of  $\eta$ , calculated for  $Q^2 = 4 \text{ GeV}^2$  and the minimal value of  $t = t_0(\eta) = -4\eta^2 M^2 / (1 - \eta^2)$ . To study the sensitivity of  $C$  on the GPD  $\tilde{H}$  we have varied the gluonic contribution, taking it as  $\tilde{H}_g = \{-1, 0, 1, 2, 3\} \cdot \tilde{H}_g^{GK}$ , where  $\tilde{H}_g^{GK}$  is given by the Goloskokov-Kroll model. On the right-hand side of Fig. 17 we show  $C$  as a function of  $t$  for  $Q^2 = 4 \text{ GeV}^2$  and  $\eta = 0.1$ . In both cases significant effects of the order of 30% are visible proving that  $C$  is a good observable sensitive to  $\tilde{H}$ .

Complementary to the studies described above, which were focused on experiments with lepton beams and fixed targets (like JLAB and COMPASS), in references [S1] and [S6] we have considered the possibility of using high energy hadron colliders as powerful sources of quasi-real photons in UltraPeripheral Collisions (UPCs) [37]. This allows the study of many aspects of photon-proton and photon-photon collisions at high energies, at RHIC but in

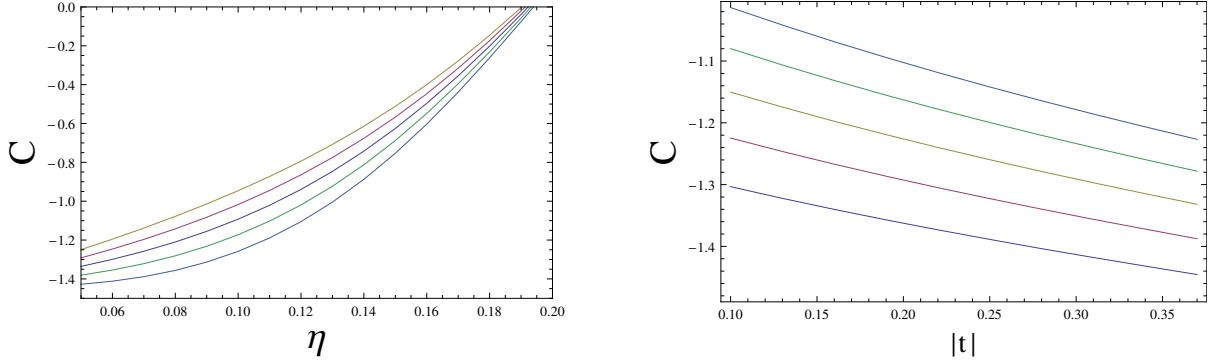


FIG. 17. (Left)  $C$  as a function of  $\eta$  calculated for  $Q^2 = 4 \text{ GeV}^2$  and  $t = t_0(\eta)$ . (Right)  $C$  as a function of  $t$  for  $Q^2 = 4 \text{ GeV}^2$  and  $\eta = 0.1$ . Different curves correspond to different polarized GPDs  $\tilde{H}_g = \{-1, 0, 1, 2, 3\} \cdot \tilde{H}_g^{GK}$ . Calculations were performed with NLO accuracy and  $\alpha_S = 0.3$ .

particular at the LHC [38]. The high luminosity and energies of these photon beams open a new kinematical domain for the study of TCS, allowing a determination of GPDs in the small skewness ( $\xi$ ) region, which is complementary to the determination at lower energy electron accelerators, such as JLab.

In [S1] we have studied the feasibility of TCS measurements in UPCs at the LHC. As described in [39] the cross section for photoproduction in proton-proton collisions is given by:

$$\sigma_{pp} = 2 \int \frac{dn(k)}{dk} \sigma_{\gamma p}(k) dk \quad (18)$$

where  $\sigma_{\gamma p}(k)$  is the cross section for the  $\gamma p \rightarrow pl^+l^-$  process and  $k$  is the photon energy. The factor  $\frac{dn(k)}{dk}$  is an equivalent photon flux (the number of photons with energy  $k$ ). The relationship between  $\gamma p$  energy squared  $s$  and  $k$  is given by:

$$s \approx 2\sqrt{s_{pp}}k,$$

where  $s_{pp}$  is the proton-proton energy squared ( $\sqrt{s_{pp}} = 14 \text{ TeV}$  for LHC).

In Fig. 18 we show the interference contribution to the cross section in comparison to Bethe-Heitler and Compton processes, for various values of photon proton energy squared  $s = 10^7 \text{ GeV}^2, 10^5 \text{ GeV}^2, 10^3 \text{ GeV}^2$ . We observe that for larger energies the Compton process dominates, whereas for  $s = 10^5 \text{ GeV}^2$  all contributions are comparable. This makes high energy collisions such as UPCs an interesting place to study TCS, as the signal (TCS) to ratio (B-H) is much better than at energies accessible at JLab or COMPASS.

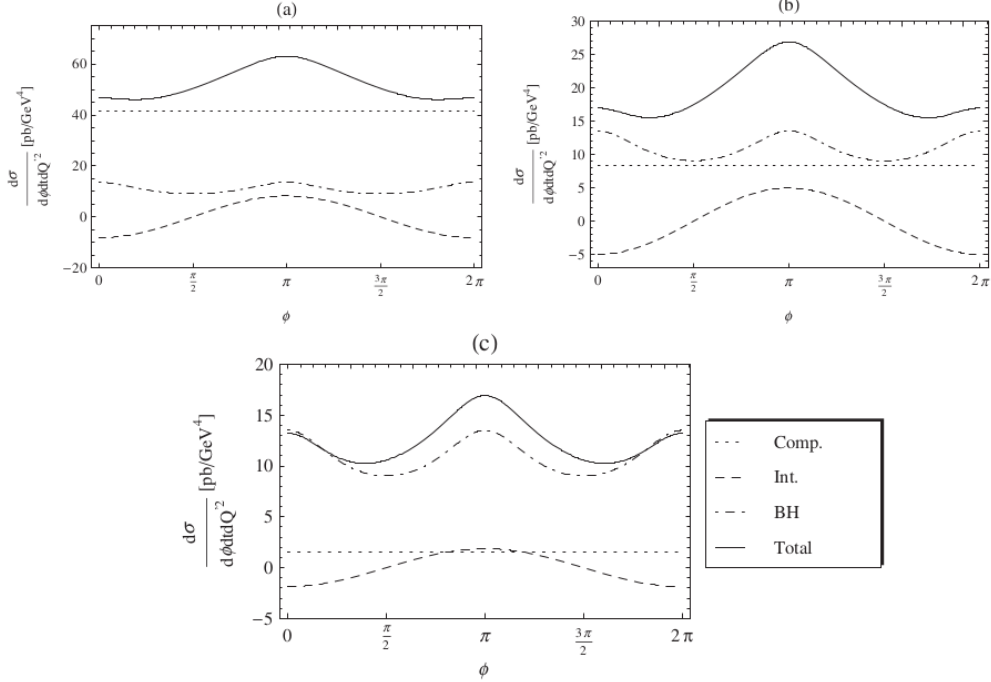


FIG. 18. The differential cross sections (solid lines) for  $t = -0.2 \text{ GeV}^2$ ,  $Q'^2 = 5 \text{ GeV}^2$  and integrated over  $\theta = [\pi/4, 3\pi/4]$ , as a function of  $\varphi$ , for  $s = 10^7 \text{ GeV}^2$  (a),  $s = 10^5 \text{ GeV}^2$  (b),  $s = 10^3 \text{ GeV}^2$  (c) with  $\mu_F^2 = 5 \text{ GeV}^2$ . We also display the Compton (dotted), Bethe-Heitler (dash-dotted) and Interference (dashed) contributions.

The pure Bethe-Heitler contribution to  $\sigma_{pp}$ , integrated over  $\theta = [\pi/4, 3\pi/4]$ ,  $\phi = [0, 2\pi]$ ,  $t = [-0.05 \text{ GeV}^2, -0.25 \text{ GeV}^2]$ ,  $Q'^2 = [4.5 \text{ GeV}^2, 5.5 \text{ GeV}^2]$ , and photon energies  $k = [20, 900] \text{ GeV}$  gives:

$$\sigma_{pp}^{BH} = 2.9 \text{ pb} . \quad (19)$$

The Compton contribution (calculated with NLO GRVGJR2008 PDFs and  $\mu_F^2 = 5 \text{ GeV}^2$ ) gives:

$$\sigma_{pp}^{TCS} = 1.9 \text{ pb} . \quad (20)$$

We have chosen the range of photon energies in accordance with proposed capabilities to tag photon energies at the LHC. This amounts to a large rate of the order of  $10^5$  events per year of data taking at the LHC with luminosity ( $10^{34} \text{ cm}^{-2}\text{s}^{-1}$ ).

In reference [S6] we have investigated the feasibility of accessing the lepton-pair production in ultraperipheral collisions at the proposed fixed-target experiment AFTER@LHC [40], which takes advantages of the multi-TeV proton and ion beams of the LHC. Table I summa-

TABLE I. Relevant parameters for  $AB$  UPCs at AFTER@LHC, at RHIC and at SPS: (i) nucleon-nucleon cms,  $\sqrt{s_{NN}}$  (ii) luminosity,  $\mathcal{L}_{AB}$ , (iii-iv) colliding hadron energies,  $E_{A,B}^{\text{lab}}$ , in the laboratory frame, (v) Lorentz factor between the colliding hadron rest frame and cms,  $\gamma = \sqrt{s_{NN}}/(2m_N)$ , (vi) Lorentz factor between both colliding hadron rest frames,  $\gamma = s_{NN}/(2m_N^2)$ , (vii-viii) inverse of the colliding hadron effective radii (giving the typical photon cloud energy in the emitter rest frame) (ix-x) photon ‘‘cutoff energy’’ in the target (resp. projectile) rest frame,  $E_{\gamma \text{ max}}^{\text{B rest}}$  (resp.  $E_{\gamma \text{ max}}^{\text{A rest}}$ ) (xi-xii) ‘‘maximum’’ photon-nucleon cms energy where  $A$  (resp.  $B$ ) is the photon emitter,  $\sqrt{s_{\gamma N}^{\text{max}}}$  (resp.  $\sqrt{s_{N\gamma}^{\text{max}}}$ ) (xiii) photon ‘‘cutoff energy’’ in the cms,  $E_{\gamma \text{ max}}^{\text{cms}}$ , with both  $A$  and  $B$  emitting a photon coherently (xiv) ‘‘maximum’’ photon-photon cms,  $\sqrt{s_{\gamma\gamma}^{\text{max}}}$ .

System	target thickness (cm)	$\sqrt{s_{NN}}$ (GeV)	$\mathcal{L}_{AB}$ ( $\text{pb}^{-1}\text{yr}^{-1}$ )	$E_A^{\text{lab}}$ (GeV)	$E_B^{\text{lab}}$ (GeV)	$\gamma^{\text{cms}}$ ( $\frac{\sqrt{s_{NN}}}{2m_N}$ )	$\gamma^{A\leftrightarrow B}$ ( $\frac{s_{NN}}{2m_N^2}$ )	$\frac{\hbar c}{R_A+R_B}$ (MeV)	$E_{\gamma \text{ max}}^{A/B \text{ rest}}$ (GeV)	$\sqrt{s_{\gamma N}^{\text{max}}}$ (GeV)	$E_{\gamma \text{ max}}^{\text{cms}}$ (GeV)	$\sqrt{s_{\gamma\gamma}^{\text{max}}}$ (GeV)
AFTER@LHC												
$pp$	100	115	$2.0 \times 10^4$	7000	$m_N$	61.0	7450	141	1050	44	8.6	17
$p\text{Pb}$	1	115	160	7000	$m_N$	61.0	7450	25.3	188	19	1.5	3.1
$pd$	100	115	$2.4 \times 10^4$	7000	$m_N$	61.0	7450	69.5	517	31	4.2	8.5
$\text{PbPb}$	1	72	$7. \times 10^{-3}$	2760	$m_N$	38.3	2940	13.9	40.7	8.8	0.53	1.1
$\text{Pbp}$	100	72	1.1	2760	$m_N$	38.3	2940	25.3	74.2	12	0.97	1.9
$\text{Arp}$	100	77	1.1	3150	$m_N$	40.9	3350	41.1	138	16	1.7	3.4
$\text{Op}$	100	81	1.1	3500	$m_N$	43.1	3720	53.0	197	19	2.3	4.6
RHIC												
$pp$	n/ap	200	12	100	100	106	22600	141	3190	77	15	30
$\text{AuAu}$	n/ap	200	$2.8 \times 10^{-3}$	100	100	106	22600	14.2	320	25	1.5	3.0
SPS												
$\text{InIn}$	n/av	17	n/av	160	$m_N$	9.23	170	16.9	2.87	2.4	0.16	0.31
$\text{PbPb}$	n/av	17	n/av	160	$m_N$	9.23	170	13.9	2.36	2.1	0.13	0.26

izes the relevant parameters characterizing ultra-peripheral collisions at AFTER@LHC, at RHIC and a SPS in fixed-target mode. We have first estimated the magnitude of the cross section for lepton-pair production from the fusion of two quasi-real photons emitted by the quasi-grazing hadrons. This purely electromagnetic BH process can serve as an important tool for the determination of the luminosities with nucleon or ion beams, but it can also be used for an experimental verification of the validity of the effective-photon approximation usually applied to estimate the flux of quasi-real photons emitted by these relativistically moving charges. Lepton-pair production also gives access to the proton GPDs via the TCS process.

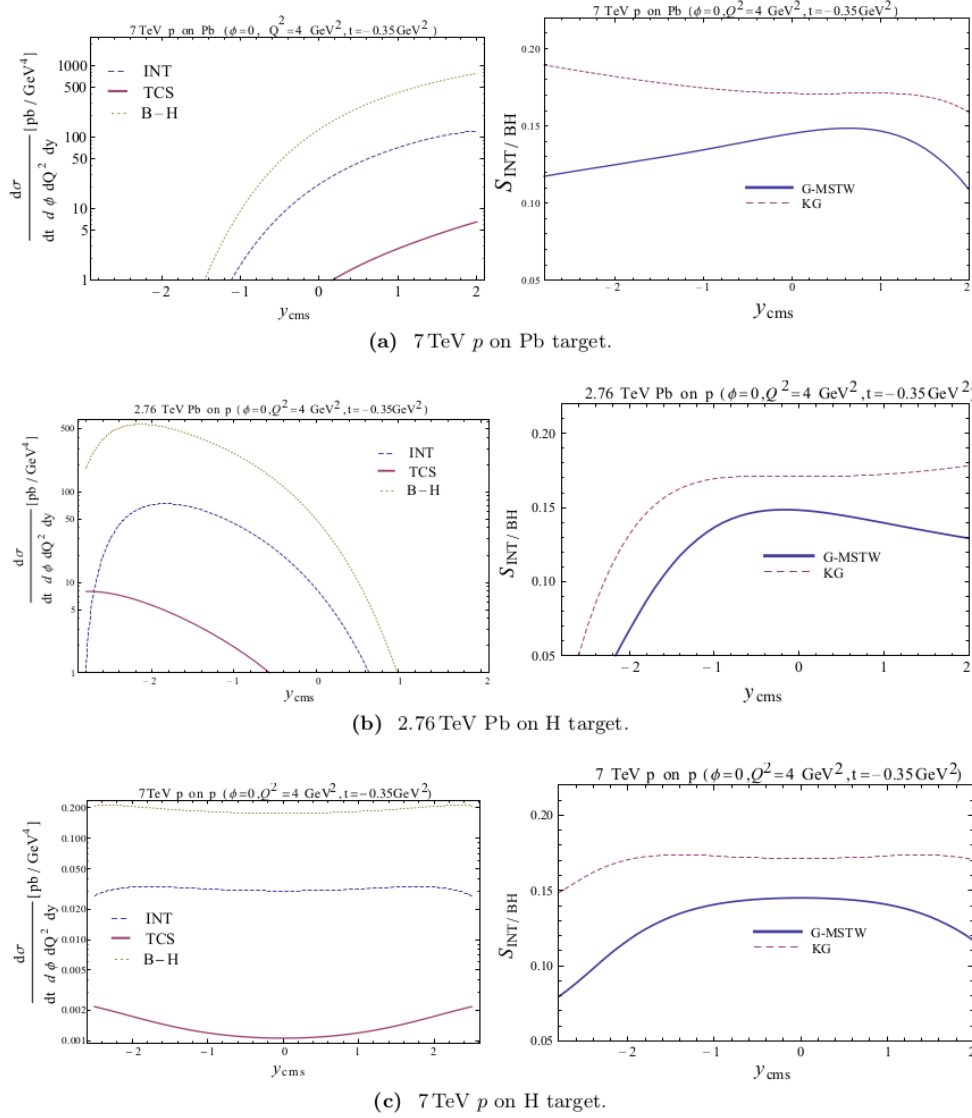


FIG. 19. (Left) Differential cross section  $\frac{d\sigma}{dydt d\phi dQ^2}$  for the GK model for  $Q^2 = 4 \text{ GeV}^2$ ,  $t = -0.35 \text{ GeV}^2$  and  $\phi = 0$  integrated over  $\theta \in (\pi/4, 3\pi/4)$ . Dotted line: B-H; dashed line: interference term; solid line: TCS. (Right) Ratio of the interference to BH differential cross section  $\frac{d\sigma}{dydt d\phi dQ^2}$  calculated for  $Q^2 = 4 \text{ GeV}^2$ ,  $t = -0.35 \text{ GeV}^2$  and  $\phi = 0$  for the GK (dashed) and G-MSTW (solid) models at NLO. From (a) to (c)  $p\text{Pb}$ ,  $\text{PbH}$  and  $p\text{H}$  cases.

The predictions that we obtained for the cross section for BH – using specific cuts relevant for the GPD extraction – are on the order of few thousand of pb for the  $p\text{Pb}$  and  $\text{Pb}p$  collisions and a slightly less than 10 pb for the  $pp$  case and we confirm the dominance of BH over TCS. This dominance can partially be overcome by studying the interference – also sensitive

on the GPDs – between TCS and BH, which we evaluated at NLO. As presented in Fig. 19, with specific cuts on the lepton polar angle, the ratio of this interference over the BH amplitude squared is on the order of 10% with two models of GPDs, used in this study i.e. GK and G-MSTW. These are quite promising values giving a hope for the extraction of the interference by means of the analysis of the azimuthal distribution of produced leptons. Studying TCS in ultraperipheral collisions at a fixed-target experiment can also give us an opportunity to study target polarization asymmetries, which are an useful tool to extract further information on GPDs [41].

Results obtained in the references [S2-S6] and experience in the analysis of the Timelike Compton Scattering process led also to the co-authorship of accepted experimental proposals for measurements at the Thomas Jefferson Accelerator Facility (JLAB):

[www.jlab.org/exp\\_prog/proposals/12/PR12-12-001.pdf](http://www.jlab.org/exp_prog/proposals/12/PR12-12-001.pdf)

[www.jlab.org/exp\\_prog/proposals/15/PR12-12-006A.pdf](http://www.jlab.org/exp_prog/proposals/15/PR12-12-006A.pdf)

##### 5. *Photoproduction of the photons pair with large invariant mass*

In the reference [S7], we have proposed and studied for the first time process of exclusive photoproduction of two photons on unpolarized proton or neutron targets:

$$\gamma(q, \epsilon) + N(p_1, s_1) \rightarrow \gamma(k_1, \epsilon_1) + \gamma(k_2, \epsilon_2) + N'(p_2, s_2), \quad (21)$$

in the kinematical regime of large invariant diphoton mass  $M_{\gamma\gamma}$  of the final photon pair and small four-momentum transfer  $t = (p_2 - p_1)^2$  between the initial and the final nucleons. Roughly speaking, these kinematics means a moderate to large, and approximately opposite, transverse momentum of each final photon. This reaction has a number of interesting features. First, it is a purely electromagnetic process at Born order (see Fig. 20) - as are deep inelastic scattering (DIS), deeply virtual Compton scattering (DVCS) and timelike Compton scattering (TCS) - and, although there is no deep understanding of this fact, this property is usually accompanied by the early scaling. Second, the process is insensitive to gluon GPDs because of the charge symmetry of the two photon final state. This may help to reduce QCD next-to-leading order corrections since they are often more important for gluon initiated partonic processes than for quark initiated ones. Third, there is also no contribution from the badly known chiral-odd quark distributions. This study enlarges the

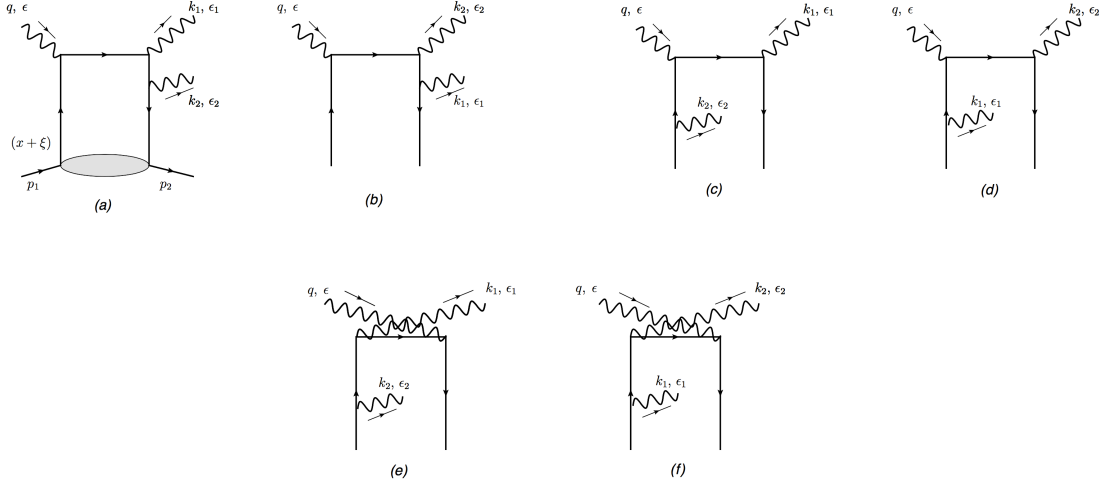


FIG. 20. Feynman diagrams contributing to the coefficient functions of the process  $\gamma N \rightarrow \gamma\gamma N'$

range of  $2 \rightarrow 3$  reactions analyzed in the framework of collinear QCD factorization [42–44].

Moreover, such process is also a good candidate to study the effects of the timelike vs spacelike nature of the probe with respect to the analytic structure of the amplitude (and to the size of the NLO corrections); since the hard scales at work in our process are both the timelike one  $M_{\gamma\gamma}^2$  and the spacelike one  $u'$ , we are facing an intermediate case between timelike Compton scattering and spacelike DVCS.

We show in Fig. 21 the differential cross section as a function of  $M_{\gamma\gamma}^2$  at  $\Delta_T = 0$  and  $S_{\gamma N} = 20 \text{ GeV}^2$ ,  $100 \text{ GeV}^2$  and  $10^6 \text{ GeV}^2$  for the photoproduction on a proton and for  $S_{\gamma N} = 20 \text{ GeV}^2$  on a neutron target. The energy dependence is moderate between JLab and COMPASS energy ranges. If we consider higher energies, we find that the cross section  $\frac{d\sigma}{dt dM_{\gamma\gamma}^2}$  decreases roughly as  $1/S_{\gamma N}$ . We understand this fact by remarking that our process does not benefit from the growth of gluon GPDs. The process is unobservable at very high energies such as those discussed in the LHeC proposal [16] with a backscattered photon beam of  $O(50 \text{ GeV})$  colliding on a 7 TeV proton beam.

The conclusion of these cross-section estimates is straightforward. This reaction can be studied at intense photon beam facilities in JLab. The rates are not very large but of comparable order of magnitude as those for the timelike Compton scattering reaction, the feasibility of which has been demonstrated [45]. Since there are no contribution from

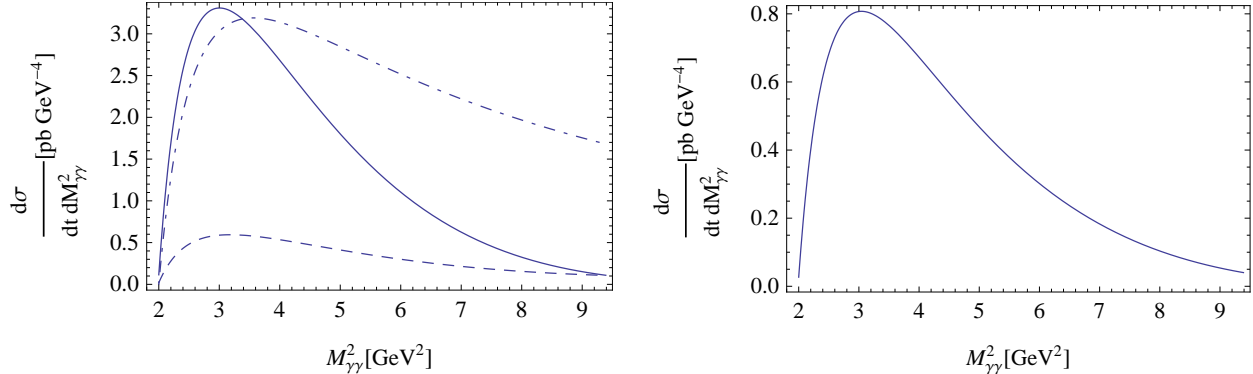


FIG. 21. The  $M_{\gamma\gamma}^2$  dependence of the unpolarized differential cross section  $\frac{d\sigma}{dM_{\gamma\gamma}^2 dt}$  on a proton (left panel) and on a neutron (right panel) at  $t = t_{min}$  and  $S_{\gamma N} = 20 \text{ GeV}^2$  (full curves),  $S_{\gamma N} = 100 \text{ GeV}^2$  (dashed curve) and  $S_{\gamma N} = 10^6 \text{ GeV}^2$  (dash-dotted curve, multiplied by  $10^5$ ). The range of integration with respect to  $u'$  is explained in the text.

gluons and sea-quarks, one does not get larger cross-sections at higher energies. Contrarily to timelike Compton scattering, it thus does not seem attractive to look for this reaction in ultra peripheral reactions at hadron colliders. We have also shown that linearly polarized real photons open the way to large asymmetries, as they do for dilepton photoproduction.

### 6. Conclusions, Impact and Outlook

The presented series of publications describes the theoretical and phenomenological developments in the description of the hard exclusive processes with a large timelike scale. Results obtained in the reference [S2] allow for next to leading order analysis of the whole family of Compton Scattering experiments: DVCS, DDVCS, TCS, which are all subject of very vivid scientific activity. Generalization of those results in the reference [S3] allowed for deriving the relation between processes with large spacelike and timelike scales at NLO, including the case of exclusive Drell-Yan process, enabling full NLO order analysis of experiments planned in the near future at J-Parc [46, 47].

In the reference [S4] we have performed the numerical analysis of the consequences of inclusion of the NLO corrections obtained in [S2] and [S3]. The important outcome of this analysis was that the gluon contributions to DVCS and TCS amplitudes and observables was much bigger, even in the moderate energy regime, than usually anticipated. This effect

is especially big in the case of the real part of the amplitude in the timelike case, which makes the observables related to it sensitive probes of the 3-dimensional gluon content of the nucleon. Such observables are going to be measured at JLAB in the experiments which were proposed by the group including the author of the presented series of publications:  
[www.jlab.org/exp\\_prog/proposals/12/PR12-12-001.pdf](http://www.jlab.org/exp_prog/proposals/12/PR12-12-001.pdf)  
[www.jlab.org/exp\\_prog/proposals/15/PR12-12-006A.pdf](http://www.jlab.org/exp_prog/proposals/15/PR12-12-006A.pdf)

In the references [S1], [S5] and [S6] we have proposed several new experimental possibilities of measurements for Timelike Compton Scattering, and finally in the ref. [S7] we introduced a new process of the photoproduction of photons pair with large invariant mass, which also depends on large timelike scale and can be measured at JLAB.

The results described in the series of papers [S1-S7] open possibilities to perform a complete NLO analysis of the exclusive processes with large timelike scales. They enable the analysis of the near future experiments, and the universality tests of the GPD formalism, without any additional assumptions regarding for example distribution amplitudes in meson production. They can be also used as an independent source for extraction of the GPDs from the data, which should give the opportunity to perform "hadron tomography", study spin structure of hadrons or even their mechanical properties [48]. Such an extraction may be performed using the PARTONS software [P3], for example along the lines of the study performed in reference [P4].

## V. DESCRIPTION OF OTHER SCIENTIFIC ACHIEVEMENTS

### A. Other important publications (after completing PhD studies)

P1 *Exclusive neutrino-production of a charmed meson*

B. Pire, L. Szymanowski, J. Wagner

Published in **Phys.Rev.D95** (2017) 094001

P2 *Hard exclusive neutrino production of a light meson*

B. Pire, L. Szymanowski, J. Wagner

Published in **Phys.Rev.D95** (2017) 114029

P3 *PARTONS: PARtonic Tomography Of Nucleon Software : A computing framework for the phenomenology of Generalized Parton Distributions*

B. Berthou, ..., J. Wagner et al..

Published in **Eur.Phys.J.C78** (2018) 478

P4 *Border and skewness functions from a leading order fit to DVCS data*

H. Moutarde, P. Sznajder, J. Wagner

Published in **Eur.Phys.J.C78** (2018) 890

P5 *Single-Transverse-Spin Asymmetries in Exclusive Photo-production of  $J/\psi$  in Ultra-Peripheral Collisions in the Fixed-Target Mode at the LHC and in the Collider Mode at RHIC*

J.P. Lansberg, L. Massacrier, L. Szymanowski, J. Wagner

Accepted for publication in **Physics Letters B**, (e-Print: arXiv:1812.04553)

In the references [P1] and [P2] we considered the cross sections for neutrino induced exclusive meson production. Neutrino production is another way to access (generalized) parton distributions [49–51]. Although neutrino induced cross sections are orders of magnitudes smaller than those for electroproduction and neutrino beams are much more difficult to handle than charged lepton beams, they have been very important to scrutinize the flavor content of the nucleon and the advent of new generations of neutrino experiments will open new possibilities. Using them would improve in a significant way future extraction of GPDs from the data.

In the reference [P1] we have focused on the production of charmed mesons. Heavy quark production allows to extend the range of validity of collinear factorization, the heavy quark mass playing the role of the hard scale. Indeed kinematics shows that the relevant scale is  $O(Q^2 + m_c^2)$ . We have demonstrated that gluon and both chiral-odd and chiral-even quark GPDs contribute in specific ways to the amplitude for different polarization states of the W. The  $y$ -dependence of the cross section allows to separate different contributions and the measurement of the azimuthal dependence, through the moments  $\langle \cos\varphi \rangle$  and  $\langle \sin\varphi \rangle$  singles out the transversity chiral-odd GPDs contributions. The flavor dependence, and in particular the difference between  $D^+$  and  $D^0$  production rates, allows to test the importance of gluonic contributions. The behaviour of the proton and neutron target cross sections enables to separate the  $u$  and  $d$  quark contributions.

Experimental data[52–56] already demonstrated their ability to distinguish different channels for charm production in neutrino and anti neutrino experiments. The statistics were however too low to separate longitudinal and transverse contributions. Moreover their analysis was not undertaken in the recent appropriate theoretical framework where skewness effects are taken into account. Planned medium and high energy neutrino facilities [57] and experiments such as *Minerva* [58] and *MINOS+* [59] which have their scientific program oriented toward the understanding of neutrino oscillations or to the discovery of the presently elusive sterile neutrinos will collect more statistics and will thus allow - without much additional equipment - some important progress in the realm of hadronic physics.

In the reference [P2] we considered hard exclusive neutrino production of a light meson: pseudoscalar  $M = \pi$  or longitudinally polarized vector  $M = \rho_L$ . Because previous studies [49] omitted the leading order gluon contributions, we update the predictions for light meson production cross sections. We have proved a very important role of gluonic GPD in the production of  $\pi^+$  mesons. Another interesting observation is that neutrino production of  $\pi$  mesons and longitudinally polarized  $\rho$  mesons are proportional at leading twist (and all orders in  $\alpha_S$ ). This is very different from the electroproduction case, where different GPDs contribute to the pseudoscalar and vector meson production amplitudes. Since the phenomenology of these two cases turned out to be very controversial [60, 61], in particular with respect to the dominance of leading twist pseudoscalar meson distribution amplitudes, the study of the neutrino case should be very informative to disentangle the role of nucleon GPDs and of meson DAs in the apparent breaking of leading twist dominance at moderate

scales.

In the reference [P3] we have described the architecture and functionalities of a C++ software framework, coined PARTONS, dedicated to the phenomenology of Generalized Parton Distributions. PARTONS provides a necessary bridge between models of Generalized Parton Distributions and experimental data collected in various exclusive production channels. We have outlined the specification of the PARTONS framework in terms of practical needs, physical content and numerical capacity. This framework will be useful for physicists - theorists or experimentalists - not only to develop new models, but also to interpret existing measurements and even design new experiments. We have described how PARTONS framework addresses the most important tasks: automation, modularity, nonregression and data storage. We have also provided examples of simple XML scenario files illustrating automated calculations of physical observables. Complete documentation with examples and detailed description of included modules is available at the PARTONS webpage [62]. We have also argued that PARTONS should become the software framework for the GPD analysis of the next-generation exclusive data. That approach was also the motivation for the workshop co-organized by author in Warsaw, during which the most active members of the community working on the GPD extraction discussed the best strategies for the next decades [63].

In the reference [P4] we have performed the global extraction of CFFs from the available proton DVCS data obtained by Hall A, CLAS, HERMES and COMPASS experiments. We use the fixed- $t$  dispersion relation technique [64] for the evaluation of CFFs at the Leading Order (LO) and Leading Twist (LT) accuracy. For a given CFF, the dispersion relation together with the analytical regularization techniques requires two components: *i*) the GPD at  $\xi = 0$ , and *ii*) the skewness ratio at  $x = \xi$ . Ansätze for those two quantities proposed in our analysis accumulate information encoded in available PDF and EFF parameterizations, and use theory developments like the  $x \rightarrow 1$  behavior of GPDs [65]. They allow to determine a border function [66, 67], being a GPD of reduced kinematic dependency  $x = \xi$ , and the subtraction constant, directly related to the energy-momentum tensor of the nucleon.

Our original approach allows to utilize many basic properties of GPDs at the level of CFFs fits. We analyze PDFs, but also EFF and DVCS data, that is, we combine information coming from (semi-)inclusive, elastic and exclusive measurements. The analysis is characterized by a careful propagation of uncertainties coming from all those sources, which we achieved with the replica method. Obtained results allow for nucleon tomography (one

of the resulting tomographic pictures is presented on Fig.3), while the extracted subtraction constant may give some insight into the distribution of forces acting on partons inside the nucleon.

The referenece [P4] was done with PARTONS [68] that is the open-source software framework for the phenomenology of GPDs. It serves not only as the main component of the fit machinery, but it is also utilized to handle multithreading computations and MySQL databases to store and retrieve experimental data. PARTONS is also used for the purpose of comparing existing models with the results of this analysis.

In reference [P5], we have evaluated the expected  $J/\psi$  photo-production cross sections for a LHCb-like detector used in fixed-target mode (AFTER@LHCb) with the 7 TeV  $p$  and 2.76 TeV Pb LHC beams and compared them to those expected at RHIC. The use of the fixed-target mode allows one to probe a very different kinematics at much larger  $x$  in the polarised nucleons.

Using a polarised-internal-gas target with a storage cell, we expect to be able to record a fraction of a million of photoproduced  $J/\psi$ 's with the  $p$  beam and about one thousand with the Pb beam. The latter case has the great advantage that the photon emitter is dominantly the Pb nucleus. With target densities about 2 orders of magnitude smaller, it seems complicated to perform such a measurement with the Pb beam without storage cell, except for the case of polarised  ${}^3\text{He}^\uparrow$  for which the injected gas flux can be increased. The latter case is particularly interesting as it allows one to probe polarised neutrons.

We have then used a model of the GPD  $E^g$  to predict the magnitue of the STSA. When folded with the expected size of the statistical samples and the target polarisation, we have found that STSAs can be measured with an absolute precision from 1 to 4 % for  $p\text{H}^\uparrow$  collisions and 10 to 30 % for  $\text{PbH}^\uparrow$  collisions. The accessible range in  $x_F$  is from 0 down to  $-0.35$  (for the  $p\text{H}^\uparrow$ ) or to  $-0.25$  (for the  $\text{PbH}^\uparrow$ ). Overall, we consider these results as a confirmation that the first measurement of the GPD  $E^g$  can be made in the fixed-target mode at the LHC by 2025.

## VI. REFERENCES

---

- [1] D. Müller, D. Robaschik, B. Geyer, F. M. Dittes, and J. Hořejši, *Fortsch. Phys.* **42**, 101 (1994), arXiv:hep-ph/9812448 [hep-ph].
- [2] X.-D. Ji, *Phys. Rev. Lett.* **78**, 610 (1997), arXiv:hep-ph/9603249 [hep-ph].
- [3] X.-D. Ji, *Phys. Rev.* **D55**, 7114 (1997), arXiv:hep-ph/9609381 [hep-ph].
- [4] A. V. Radyushkin, *Phys. Lett.* **B385**, 333 (1996), arXiv:hep-ph/9605431 [hep-ph].
- [5] A. V. Radyushkin, *Phys. Rev.* **D56**, 5524 (1997), arXiv:hep-ph/9704207 [hep-ph].
- [6] M. Burkardt, *Phys. Rev.* **D62**, 071503 (2000), [Erratum: *Phys. Rev.* **D66**, 119903 (2002)], arXiv:hep-ph/0005108 [hep-ph].
- [7] M. Burkardt, *Int. J. Mod. Phys.* **A18**, 173 (2003), arXiv:hep-ph/0207047 [hep-ph].
- [8] M. Burkardt, *Phys. Lett.* **B595**, 245 (2004), arXiv:hep-ph/0401159 [hep-ph].
- [9] H. Moutarde, P. Sznajder, and J. Wagner, *Eur. Phys. J.* **C78**, 890 (2018), arXiv:1807.07620 [hep-ph].
- [10] L. Favart, M. Guidal, T. Horn, and P. Kroll, *Eur. Phys. J.* **A52**, 158 (2016), arXiv:1511.04535 [hep-ph].
- [11] N. d’Hose, S. Niccolai, and A. Rostomyan, *Eur. Phys. J.* **A52**, 151 (2016).
- [12] P. Kroll, H. Moutarde, and F. Sabatie, *Eur. Phys. J.* **C73**, 2278 (2013), arXiv:1210.6975 [hep-ph].
- [13] J. Dudek *et al.*, *Eur. Phys. J.* **A48**, 187 (2012), arXiv:1208.1244 [hep-ex].
- [14] F. Gautheron *et al.*, “*COMPASS-II Proposal*,” (2010), SPSC-P-340, CERN-SPSC-2010-014.
- [15] A. Accardi *et al.*, *Eur. Phys. J.* **A52**, 268 (2016), arXiv:1212.1701 [nucl-ex].
- [16] J. L. Abelleira Fernandez *et al.*, *J. Phys.* **G39**, 075001 (2012), arXiv:1206.2913 [physics.acc-ph].
- [17] E. R. Berger, M. Diehl, and B. Pire, *Eur. Phys. J.* **C23**, 675 (2002), arXiv:hep-ph/0110062 [hep-ph].
- [18] G. Altarelli, R. K. Ellis, and G. Martinelli, *Nucl. Phys.* **B157**, 461 (1979).
- [19] R. Stroyanowski, *Phys. Rept.* **71**, 1 (1981).
- [20] M. Guidal and M. Vanderhaeghen, *Phys. Rev. Lett.* **90**, 012001 (2003), arXiv:hep-ph/0208275

- [hep-ph].
- [21] X.-D. Ji and J. Osborne, Phys. Rev. **D58**, 094018 (1998), arXiv:hep-ph/9801260 [hep-ph].
- [22] L. Mankiewicz, G. Piller, E. Stein, M. Vanttinen, and T. Weigl, Phys. Lett. **B425**, 186 (1998), [Erratum: Phys. Lett.B461,423(1999)], arXiv:hep-ph/9712251 [hep-ph].
- [23] A. V. Belitsky and D. Mueller, Phys. Lett. **B417**, 129 (1998), arXiv:hep-ph/9709379 [hep-ph].
- [24] A. V. Belitsky, D. Mueller, L. Niedermeier, and A. Schafer, Phys. Lett. **B474**, 163 (2000), arXiv:hep-ph/9908337 [hep-ph].
- [25] K. Kumerički and D. Mueller, Nucl. Phys. **B841**, 1 (2010), arXiv:0904.0458 [hep-ph].
- [26] S. V. Goloskokov and P. Kroll, Eur. Phys. J. **C50**, 829 (2007), arXiv:hep-ph/0611290 [hep-ph].
- [27] D. Boer *et al.*, (2011), arXiv:1108.1713 [nucl-th].
- [28] W. Schafer, G. Slipek, and A. Szczurek, Phys. Lett. **B688**, 185 (2010), arXiv:1003.0610 [hep-ph].
- [29] A. V. Radyushkin, Phys. Rev. **D59**, 014030 (1999), arXiv:hep-ph/9805342 [hep-ph].
- [30] M. Diehl, Phys. Rept. **388**, 41 (2003), arXiv:hep-ph/0307382 [hep-ph].
- [31] S. V. Goloskokov and P. Kroll, Eur. Phys. J. **C42**, 281 (2005), arXiv:hep-ph/0501242 [hep-ph].
- [32] S. V. Goloskokov and P. Kroll, Eur. Phys. J. **C53**, 367 (2008), arXiv:0708.3569 [hep-ph].
- [33] A. D. Martin, W. J. Stirling, R. S. Thorne, and G. Watt, Eur. Phys. J. **C63**, 189 (2009), arXiv:0901.0002 [hep-ph].
- [34] A. Bacchetta, U. D’Alesio, M. Diehl, and C. A. Miller, Phys. Rev. **D70**, 117504 (2004), arXiv:hep-ph/0410050 [hep-ph].
- [35] M. Battaglieri *et al.*, “*Meson spectroscopy with low- $Q^2$  electron scattering in CLAS12,*” (2012), PR12-11-005.
- [36] A. Somov (GlueX), *Proceedings, 12th International Conference on Meson-nucleon physics and the structure of the nucleon (MENU 2000): Williamsburg, USA, May 31-June 4, 2010*, AIP Conf. Proc. **1374**, 282 (2011).
- [37] G. Baur, K. Hencken, D. Trautmann, S. Sadovsky, and Y. Kharlov, Phys. Rept. **364**, 359 (2002), arXiv:hep-ph/0112211 [hep-ph].
- [38] A. J. Baltz, Phys. Rept. **458**, 1 (2008), arXiv:0706.3356 [nucl-ex].
- [39] C. A. Bertulani, S. R. Klein, and J. Nystrand, Ann. Rev. Nucl. Part. Sci. **55**, 271 (2005), arXiv:nucl-ex/0502005 [nucl-ex].
- [40] S. J. Brodsky, F. Fleuret, C. Hadjidakis, and J. P. Lansberg, Phys. Rept. **522**, 239 (2013),

- arXiv:1202.6585 [hep-ph].
- [41] M. Boër, M. Guidal, and M. Vanderhaeghen, (2015), arXiv:1501.00270 [hep-ph].
- [42] M. El Beiyad, B. Pire, M. Segond, L. Szymanowski, and S. Wallon, Phys. Lett. **B688**, 154 (2010), arXiv:1001.4491 [hep-ph].
- [43] D. Yu. Ivanov, B. Pire, L. Szymanowski, and O. V. Teryaev, Phys. Lett. **B550**, 65 (2002), arXiv:hep-ph/0209300 [hep-ph].
- [44] S. Kumano, M. Strikman, and K. Sudoh, Phys. Rev. **D80**, 074003 (2009), arXiv:0905.1453 [hep-ph].
- [45] M. Boër, M. Guidal, and M. Vanderhaeghen, Eur. Phys. J. **A51**, 103 (2015).
- [46] T. Sawada, W.-C. Chang, S. Kumano, J.-C. Peng, S. Sawada, and K. Tanaka, Phys. Rev. **D93**, 114034 (2016), arXiv:1605.00364 [nucl-ex].
- [47] J. Ahn *et al.*, “Letter of intent: Studying generalized parton distributions with exclusive drell-yan process at j- parc,” (2018).
- [48] M. V. Polyakov and P. Schweitzer, Int. J. Mod. Phys. **A33**, 1830025 (2018), arXiv:1805.06596 [hep-ph].
- [49] B. Z. Kopeliovich, I. Schmidt, and M. Siddikov, Phys. Rev. **D86**, 113018 (2012), arXiv:1210.4825 [hep-ph].
- [50] B. Lehmann-Dronke and A. Schafer, Phys. Lett. **B521**, 55 (2001), arXiv:hep-ph/0107312 [hep-ph].
- [51] A. Psaker, W. Melnitchouk, and A. V. Radyushkin, Phys. Rev. **D75**, 054001 (2007), arXiv:hep-ph/0612269 [hep-ph].
- [52] N. Ushida *et al.* (Fermilab E531), Phys. Lett. **B206**, 375 (1988).
- [53] S. A. Rabinowitz *et al.*, Phys. Rev. Lett. **70**, 134 (1993).
- [54] P. Vilain *et al.* (CHARM II), Eur. Phys. J. **C11**, 19 (1999).
- [55] P. Astier *et al.* (NOMAD), Phys. Lett. **B486**, 35 (2000).
- [56] A. Kayis-Topaksu *et al.*, New J. Phys. **13**, 093002 (2011), arXiv:1107.0613 [hep-ex].
- [57] D. S. Ayres *et al.* (NOvA), (2004), arXiv:hep-ex/0503053 [hep-ex].
- [58] L. Aliaga *et al.* (MINERvA), Nucl. Instrum. Meth. **A743**, 130 (2014), arXiv:1305.5199 [physics.ins-det].
- [59] A. Timmons, Adv. High Energy Phys. **2016**, 7064960 (2016), arXiv:1511.06178 [hep-ex].
- [60] S. V. Goloskokov and P. Kroll, Eur. Phys. J. **C65**, 137 (2010), arXiv:0906.0460 [hep-ph].

- [61] S. V. Goloskokov and P. Kroll, Eur. Phys. J. **A47**, 112 (2011), arXiv:1106.4897 [hep-ph].
- [62] "PARTONS web page," <https://www.partons.cea.fr>.
- [63] "Prospects for extraction of gpdfs from global fits of current and future data." <https://events.ncbj.gov.pl/e/gpd2019>.
- [64] O. V. Teryaev, in *11th International Conference on Elastic and Diffractive Scattering: Towards High Energy Frontiers: The 20th Anniversary of the Blois Workshops, 17th Rencontre de Blois (EDS 05) Chateau de Blois, Blois, France, May 15-20, 2005* (2005) arXiv:hep-ph/0510031 [hep-ph].
- [65] F. Yuan, Phys. Rev. **D69**, 051501 (2004), arXiv:hep-ph/0311288 [hep-ph].
- [66] A. V. Radyushkin, Phys. Rev. **D83**, 076006 (2011), arXiv:1101.2165 [hep-ph].
- [67] A. V. Radyushkin, *Proceedings, QCD Evolution Workshop (QCD 2012): Newport News, Virginia, USA, May 14-17, 2012*, Int. J. Mod. Phys. Conf. Ser. **20**, 251 (2012).
- [68] B. Berthou *et al.*, Eur. Phys. J. **C78**, 478 (2018), arXiv:1512.06174 [hep-ph].

Jakob Wagner